Non-invasive measure of heat stress in sheep using machine learning techniques and infrared thermography

A. Joy[1*], S. Taheri[1], F.R. Dunshea[1,2], B.J. Leury[1], K. DiGiacomo[1], R. Osei- Amponsah [1,3], G. Brodie[1], and S. S. Chauhan[1]

[1] School of Agriculture and Food, The University of Melbourne, Parkville, VIC 3010, Australia
[2]Faculty of Biological Sciences, The University of Leeds, Leeds LS2 9JT, United Kingdom
[3]Department of Animal Science, School of Agriculture, University of Ghana, Legon, Ghana

*Corresponding author: aleenajoyj@student.unimelb.edu.au

Abstract

Heat stress (HS) leads to altered sheep behavior, physiological, and biochemical processes which negatively affects their welfare and performance. While suitable strategies are needed to ameliorate the impacts of HS in sheep, it is equally important to accurately and non-invasively measure HS. Traditionally, rectal temperature (RT) is considered an indicator of thermal balance and is used to assess the impacts of hot conditions on sheep. However, measuring RT itself can be a stressor as it often requires restraining of the animals. The main objective of this study was to establish whether a combination of infrared thermography (IRT) and machine learning techniques can be applied to predict sheep RT when subjected to HS. Thermal images and RT were taken twice weekly from Dorper, and 2nd Cross (Poll Dorset X (Border Leicester X Merino)) lambs (n=24/breed, 4-5 months old), for two weeks. Sheep were randomly allocated to either (i) thermoneutral (TN; 18–21 °C, 30–50% relative humidity (RH), n = 12/group) or (ii) cyclic HS treatments (28–40 °C, 40-60% RH, the cycle comprised of high temperatures 38-40 °C between 0800 and 1700 h daily and 28 °C, 30-40% RH maintained overnight). The head was selected as the region of interest because of less wool cover; specifically, the IRT of forehead, eye, ear, nostril, and face locations were measured. Artificial neural network (ANN) models were developed using three different backpropagation algorithms with temperature-humidity index (THI), and IRT temperatures as inputs and RT measured manually as targets. Results showed that the forehead and eye IRT temperatures had the highest correlation ($P<0.01$) with THI and RT. Further, Bayesian Regularization, with one hidden layer containing 10 neurons with a tangent sigmoid transfer function, showed the best correlation ($R=0.92$) and highest performance ($MSE=0.02$). The model developed may be a rapid and cost-effective technique to monitor real-time body temperatures in sheep and also to detect HS with minimal restraint.

Keywords: heat stress, infrared thermography, machine learning, rectal temperature

Introduction

Excessive heat load or heat stress (HS) describes a situation where the thermoregulatory mechanisms of an animal fail to regulate the body temperature effectively within the normal range. HS is a major constraint to the wellbeing and productivity of farm animals, such as sheep reared under subtropical and tropical conditions (Marai et al., 2008; Joy et al., 2020a; Baida et al., 2021). The primary physiological response to HS in ruminants involves increased body temperature and respiration rate (normal body temperature and respiration rate range in sheep is 38.1-39.9 ºC and 12-30 beats/min; but the values may vary under different conditions such as level of activity, diet, breed and age) (Chauhan et al., 2014b; Joy et al., 2020b). Prolonged heat stress often leads to low productivity (Koluman and Daskiran, 2011; Maurya et al., 2016), compromised immune function (Chauhan et al., 2014a; Shi et al., 2020; Chauhan et al., 2021), high morbidity, and mortality (Phillips, 2016). Early identification of animals under moderate /extreme HS is vital to enable suitable interventions such as providing access to shade, cool drinking water and in severe cases artificial cooling of stressed animals using pedestal fans to mitigate HS, improve animal welfare, and reduce the risk of sheep mortality. However, systematic screening to identify signs of HS is particularly difficult under farm conditions, especially in grazing systems, where animals are present in large numbers. Although weather indices such as temperature-humidity index (THI) and heat load index (HLI) could act as a guide for estimating HS severity in livestock, they carry a set of limitations. The primary constraint for using bioclimatic indices is their poor relationship to the thermoregulatory dynamics of the animals under excessive HS. Typically, the level of HS in animal depends upon the inherent genetic potential of the individual animal to the stressful conditions, which may vary for species, breed, age, physiological stage etc. (Osei-Amponsah et al., 2019; Joy et al., 2020a). Therefore, irrespective of the available information, methods to measure and monitor the physiological responses such as body temperature in real-time may give more information on the early detection of HS in sheep.

The animal's core body temperature estimates the temperature of vital internal organs such as the heart, liver, and brain. There are several indicators established in ruminants as an indirect measurement to represent core body temperature comprising rectal (Goodwin, 1998), vaginal (Hillman et al., 2009), tympanic (Brown-Brandl et al., 1999) and rumen temperature (Ipema et al., 2008; Lees et al., 2019). Among those, rectal temperature (RT) is used as a conventional "gold standard" indicator of core body temperature in sheep. Nevertheless, measurements of RT are time-consuming, labor-intensive, and often require manual handling, which can affect animal welfare. Infrared thermography (IRT) provides an alternative approach for quantifying animal body temperature. This approach measures the surface temperature based on proportional emissions of heat radiation from the body (Salles et al., 2016; Macmillan et al., 2019). Infrared images also indicate the difference in the blood flow resulting from high body temperature under stressful environmental conditions (McManus et al., 2015). Hence, the temperature of different body locations such as the eye (Hoffmann et al., 2013; Daltro et al., 2017), fore-head (Peng et al., 2019), muzzle (Fuentes et al., 2020b), rump (Baida et al., 2021), flank (McManus et al., 2015), feet (Montanholi et al., 2008) and udder temperatures (Metzner et al., 2014; Osei-Amponsah et al., 2020), measured using IRT, have been used to quantify physiological parameters and stress in various livestock species. Thermal imaging is fast, reliable and has the advantage that it could screen many animals with little or no restraint (Idris et al., 2021). Also, this method is more advanced, non-invasive and has greater potential for automation than conventional methods (Salles et al., 2016; Fuentes et al., 2020b). However, there are some limitations and factors that must be taken into consideration while using IRT. Accurate measurement of IRT often requires a consistent image angle and distance to the subject, along with constant ambient temperature, wind speed, and direct sunlight (Idris et al., 2021). Also, it is not possible to predict RT from IRT imaging. However, a model could be developed to predict it from the surface temperatures of the body and because of non-linearity of the relation between the inputs and the target, machine learning could provide a more accurate prediction.

Machine learning and computer vision algorithms provide new opportunities to non-invasively examine farm animals in terms of behavior (Stewart et al., 2017; Fuentes et al., 2020a), physiology (Jorquera-Chavez et al., 2019; Fuentes et al., 2020b), and production changes (Fuentes et al., 2020c). Artificial neural networks (ANN) are widely applied in multiple agricultural fields, designed to learn, and find patterns among the input data to predict specific outputs (Gonzalez Viejo et al., 2019; Taheri et al., 2021). Model development is achieved by a process of training where these algorithms process the data by modifying weights and biases to obtain the best correlation (Taheri et al., 2021). Applications of IRT and ANN have been recently implemented to analyze environmental-related stress responses in farm animals based on changes in body temperature (Jorquera-Chavez et al., 2019; Fuentes et al., 2020b). However, using the ANN technique usually requires selecting the best neural network structure with optimum model factors such as the number of hidden layers, neurons, training function, and the activation function for hidden layers and the output function (Taheri et al., 2021). A hidden layer is located between the input and output of the algorithm, in which the function applies weights to the inputs and directs them through an activation function as the output. The number of hidden layers and neurons is mostly determined by trial-and-error to obtain the best model with a minimum error and high performance in predicting the target values (Gonzalez Viejo et al., 2019). Compared to other ruminant species (cattle and goats), sheep have thick wool that acts as a significant resistance layer to the skin (Fuentes et al., 2020b). We propose that the facial area of the head would be suitable for measuring skin temperature using IRT as this location contains minimal wool in sheep. Therefore, the main objective of this research was to explore the correlations between the temperatures obtained from IRT images of a sheep's head and develop an ANN model to predict the RT using these images.

Materials and Methods

Animals and Experimental Design

The live animal study was approved by the Faculty of Veterinary and Agricultural Sciences, The University of Melbourne Animal Ethics Committee (Ethics ID: 1714357.1) and was conducted at The University of Melbourne, Dookie Campus, Victoria, Australia (36°23'01.9"S 145°42'52.1"E) over two weeks. The details on animals and experimental design have been previously reported by Joy et al. (2020b) and Zhang et al. (2021). Briefly, 48 lambs of two different breeds, Dorper and 2nd Cross [SC; Poll Dorset X (Border Leicester X Merino)] lambs (24 lambs from each breed; 4-5 months old with live weight = 40.9 ± 0.91 kg, (Mean ± SD) were used in the study. The lambs were acclimatized to indoor facilities for two weeks before starting the measurements. They were fed a mixed ration (50% pellets, 25% oaten hay, and 25% lucerne chaff) *ad libitum*, complimented with freshwater *ad libitum*. After acclimatization, lambs were randomly allocated to two treatments (i) thermoneutral (TN; 18–21 °C, 30–50% relative humidity (RH), n = 12/group) and (ii) cyclic heat stress (HS; 28–40 °C, 40-60% RH, the cycle comprised of high temperatures 38-40 °C between 800 and 1700 h daily and 28 °C, 30-40% RH maintained overnight).

Data Acquisition

During the current study, the temperature and RH of the treatment rooms (TN and HS) were recorded at 30-minute intervals using a universal serial bus (USB) temperature and humidity data logger (TechBrands; Electus Distribution, Rydalmere, NSW, Australia). Based on the weather variables, the THI was calculated according to the formula described by Marai et al. (2007), given T and RH as dry-bulb temperature (°C) and relative humidity (%) respectively.

$$\mathrm{THI} = \mathrm{T} - \{(0.31 - 0.0031 * \mathrm{RH}) * (\mathrm{T} - 14.4)\}. \quad \ldots (1)$$

Thermal images were obtained twice weekly at 1700 h using a handheld portable infrared thermal camera FLIR T1050sc (FLIR Systems Inc.; Wilsonville, OR, USA) with thermal sensitivity of <20 mK and a wide temperature range (-40 °C to +2000 °C). The camera has an accuracy of ±2 °C or ±2% of reading at 25 °C for temperatures up to 1200 °C, with an emissivity of 0.985 (FLIRSystems, 2015; Osei-Amponsah et al., 2020). Sheep were restrained in a standing position and thermal imaging was performed at approximately 0.5 m distance from the animal at an angle of between 30° to 40° with emissivity set to 0.95, as indicated for animal skin (Stelletta et al., 2012). Thermal images were analyzed using the FLIR's ResearchIR Max software (FLIRSystems, 2015) to record the skin temperature of the lambs in various body locations. Specifically, the head was selected as a region of interest (ROI) for temperature estimation as this area contains less wool and other regions of the body may create a bias for data extraction between hair and wool sheep breeds (Fuentes et al., 2020b). Henceforth, nostril (nostril T), forehead (FH T), ear (ear T), eye (eye T), and face (face T) were selected as ROIs for this current study (Fig 1). One of the main constraints in extracting FH T from SC lambs was that they had less wool in the forehead region which may create biases in the data obtained. Therefore, FH T on both breeds were obtained from a slighter lower location, level with the eye to avoid any interruptions from wool (Fig 1). The RT of the animals was also simultaneously measured using a digital thermometer (Model: DT-K11A; Honsun, Shanghai, China).

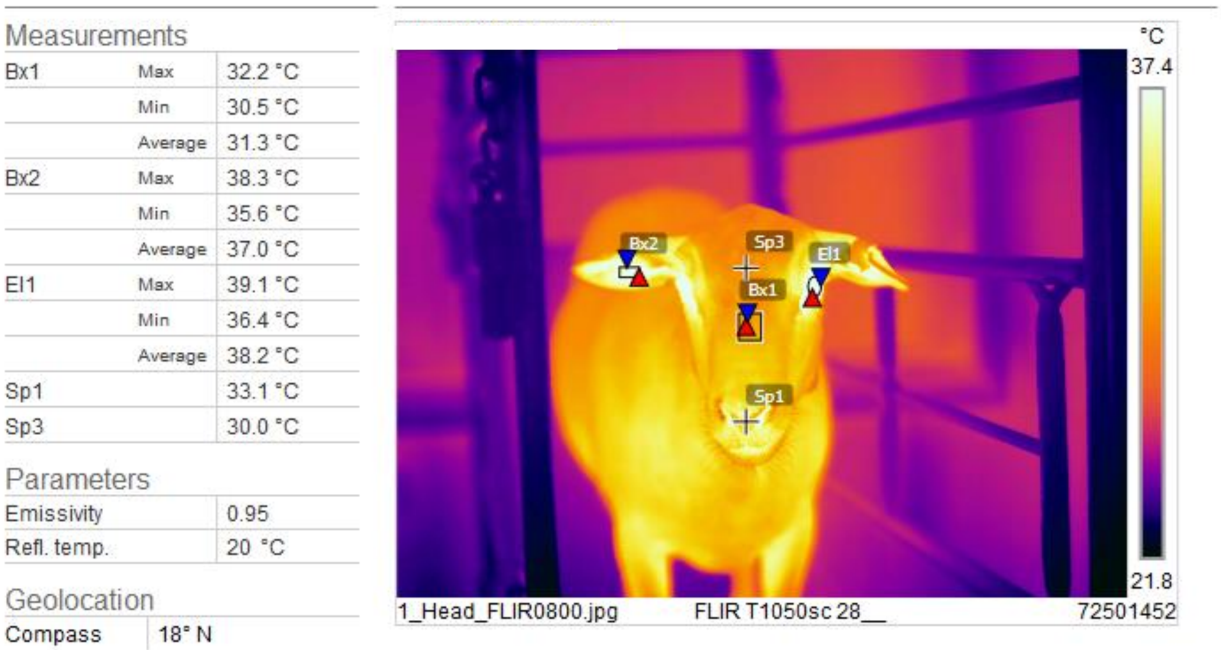

Fig 1. Example of a thermal image of a Dorper sheep's head showing the region of interests (ROIs) selected; Bx1- Face, Bx2- Ear, EI1- Eye, Sp1- Nostril and Sp3- Fore-head

Artificial Neural Network (ANN) modeling

ANN model structure

The basic structure of an ANN model consists of an input layer, one or more hidden layers, and an output layer. In every layer, there are several nodes, or neurons, with each layer using the output of the preceding layer as its input, so neurons interconnect with distinct layers. Each neuron specifically has weights that are modified during the learning process, and as the weight decreases or increases, it adjusts the strength of the signal of that neuron (Taheri et al., 2021). In this current study, the model was constructed based on a two-layer feedforward network with a tan-sigmoid activation function in the hidden layer and a linear transfer function in the output layer. Fig 2 illustrates the graphical representation of the entire study design. The input variables selected for the prediction of RT were forehead, eye, ear, nostril, and overall face temperature obtained from infrared thermography, THI and breed type (represented as binary numbers; Dorper and SC as 0,1 respectively). The neural fitting app of MATLAB 2020a (MathWorks Inc., Natick, MA, USA) allows for selecting data, creating, and training a network and validating its performance using correlation coefficient (R) and mean square error (MSE) as the goodness of fit criteria. Three back-propagation training algorithms (Levenberg-Marquardt, Bayesian Regularization (BR), and Scaled

Conjugate Gradient) were used to train the ANN model to predict RT in sheep. A neuron trimming exercise (5, 7, 10 and 15 neurons) was performed to obtain the best-hidden layer structure based on the highest accuracy (highest R and lowest MSE) for each algorithm (data not shown). Fifteen was the highest number of neurons considered for all the models because the use of a large number of neurons would most likely result in overfitting (Gonzalez Viejo et al., 2019). The original dataset, corresponding to 192 observations, was randomly divided into 70% for training (N=134), 15% for testing (N=29) and 15% for validation (N=29) for each model. In the BR algorithm, 85% of the data was applied for training and 15% for testing. This algorithm has an implemented cross-validation, which is performed on the training data (85%).

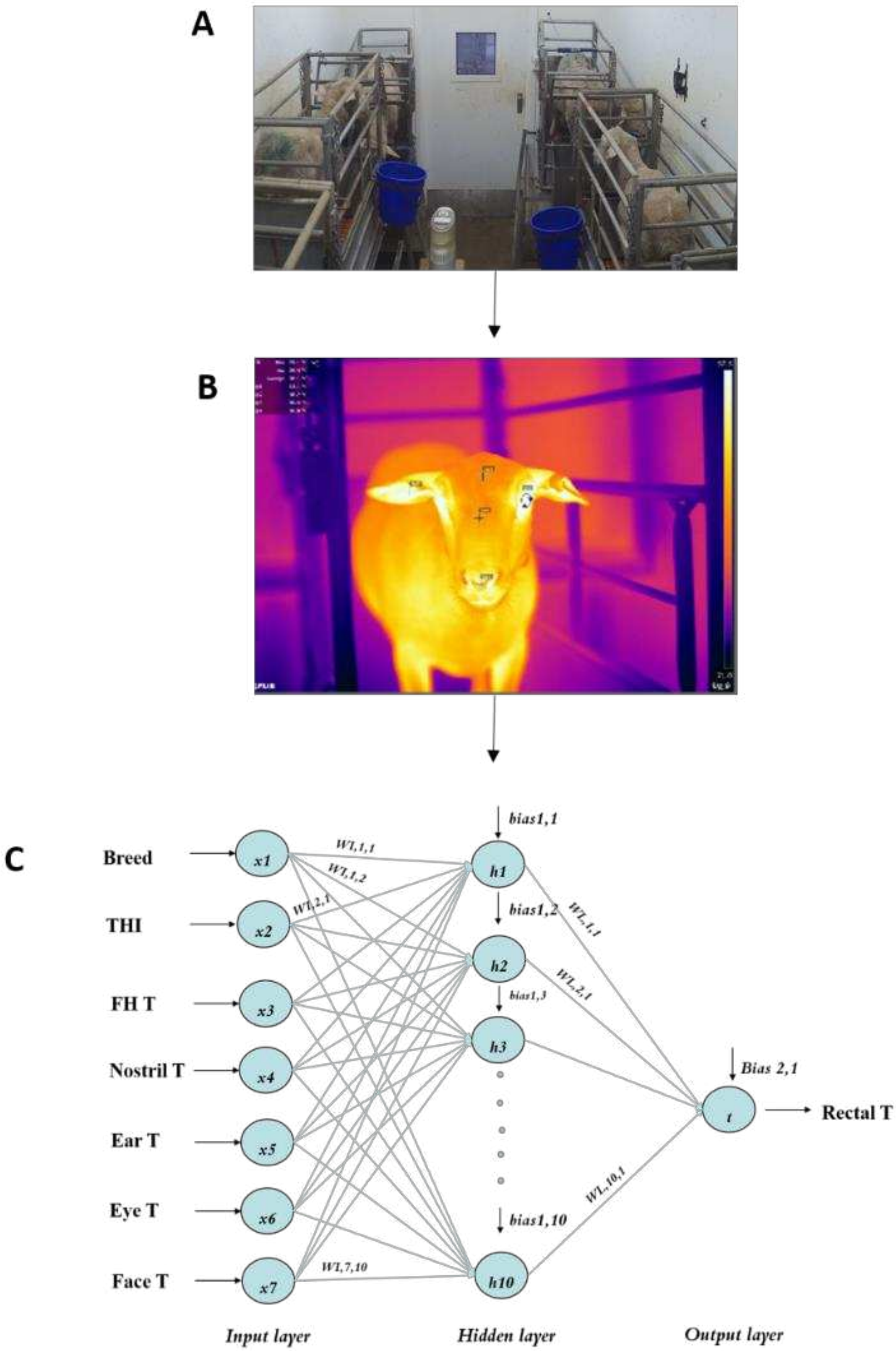
A
B
C
Breed
THI
FH T
Nostril T
Ear T
Eye T
Face T
x1
x2
x3
x4
x5
x6
x7
WI,1,1
WI,1,2
WI,2,1
WI,7,10
bias1,1
bias1,2
bias1,3
bias1,10
h1
h2
h3
h10
WL,1,1
WL,2,1
WL,10,1
Bias 2,1
t
Rectal T
Input layer
Hidden layer
Output layer

Fig 2. Graphical representation of the study design: (A) the experimental layout, (B) the thermal image capturing and processing with the selected region of interests in the head and extraction of temperature (°C) values from the infrared thermal image (IRTI) analysis, (C) the schematic illustration of artificial neural network model to predict rectal temperature. Model diagram abbreviations: THI: temperature-humidity index; T: temperature; w: weights.

Statistical analysis

The correlation among THI, RT and skin temperatures (obtained from IRTs) were estimated using correlation analysis in Genstat (GenStat 19th Edition; VSN International Ltd., Hemel Hempstead, UK) with a significance level set at $P \leq 0.05$. Further, the statistical analysis to evaluate and compare the accuracy of the developed models consisted of R, MSE to assess performance and slope for each of the (i) training, (ii) validation, (iii) testing, and (iv) overall model stages. For the best model, the percentage of outliers using 95% confidence boundary was calculated. Linear regression analysis for temperature data with the intercept passing through the origin and $P \leq 0.05$ as the criteria were used to compare the RT measurements using the manual methods against the predicted RT using the ANN model with Minitab® 19 (Penn State University, PA, USA).

Dimension reduction using principal component analysis (PCA) was performed in Minitab to find relationships and patterns among the data between THI, manual RT measurements, skin temperatures obtained from IRTs and estimated RT using the ANN model proposed. Both breed type and THI were also included in PCA analysis.

Results

The THI values calculated for the study period (2 weeks) ranged from 19.2-21.8 for TN conditions to 26.5-35.3 for HS treatment (Fig 3A) (Joy et al., 2020b).

(A)

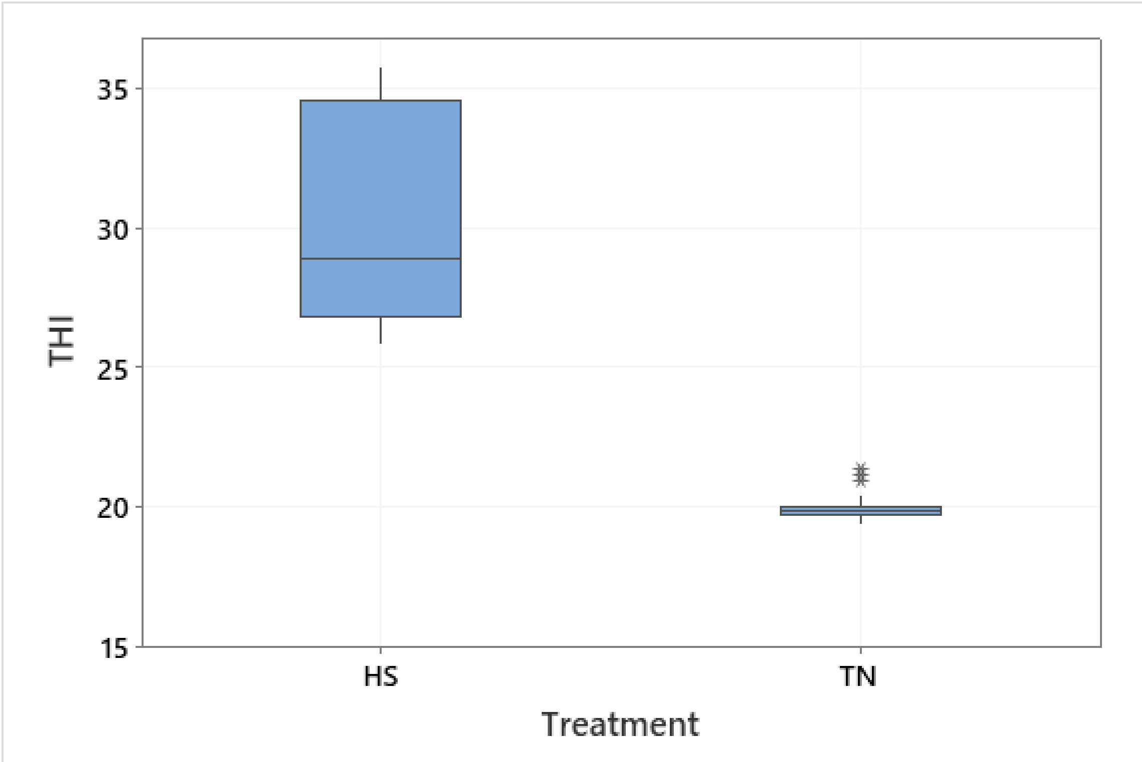
THI
35
30
25
20
15
HS
TN
Treatment

(B)

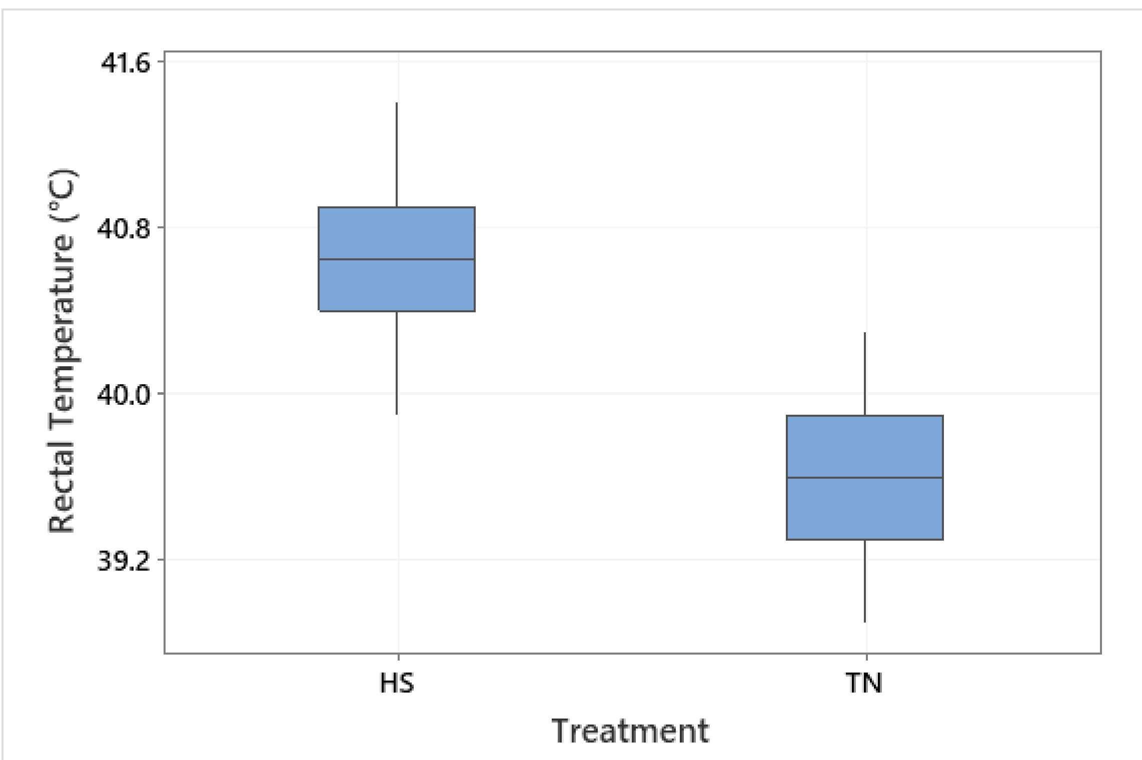
Rectal Temperature (°C)
41.6
40.8
40.0
39.2
HS
TN
Treatment

Fig 3. Boxplots showing (A) THI and (B) RT values for both TN and HS treatments over two weeks

Table 1 shows the correlations between THI, RT, and skin temperatures (forehead, eye, ear, nostril, and face region) obtained from IRT. Overall, skin temperatures obtained from IRT showed a positive correlation (P<0.01) with THI and RT in the afternoon. Among various ROIs selected, FH T (R=0.84; P<0.01) and eye T (R=0.68; P<0.01) had the highest correlation with THI. Significant positive correlations (P<0.01) were also obtained between RT and FH T, nostril T and eye T (R=0.68, 0.58, 0.52 respectively; Table 1). Since, sheep head surface temperatures, measured using IRT, had a positive correlation (P<0.01) with RT, they were all considered as inputs for model development.

Table 1. Pearson correlation coefficients between THI, RT and skin temperatures (Forehead, eye, ear, nostril and face) in sheep (n=192)

	THI	**RT**	**FH T**	**Eye T**	**Ear T**	**Nostril T**	**Face T**
THI	1						
RT	0.81**	1					
FH T	0.85**	0.68**	1				
Eye T	0.60**	0.67**	0.66**	1			
Ear T	0.56**	0.65**	0.65**	0.78**	1		
Nostril T	0.62**	0.55**	0.75**	0.72**	0.74**	1	
Face T	0.68**	0.50**	0.46**	0.72**	0.73**	0.48**	1

THI: Temperature-humidity index; RT: rectal temperature; FH T: fore-head temperature; Eye T: Eye temperature; Ear T: Ear temperature; Nostril T: Nostril temperature; Face T: Face temperature. **correlation differs (P<0.01) from zero.

Figure 4 shows the linear regression between RT measured manually and predicted using Bayesian training algorithm with THI as the input variable. As depicted, the correlation and determination coefficients were relatively low (R=0.81, R^2= 0.66; P<0.001) with MSE=0.16 and slope=0.68.

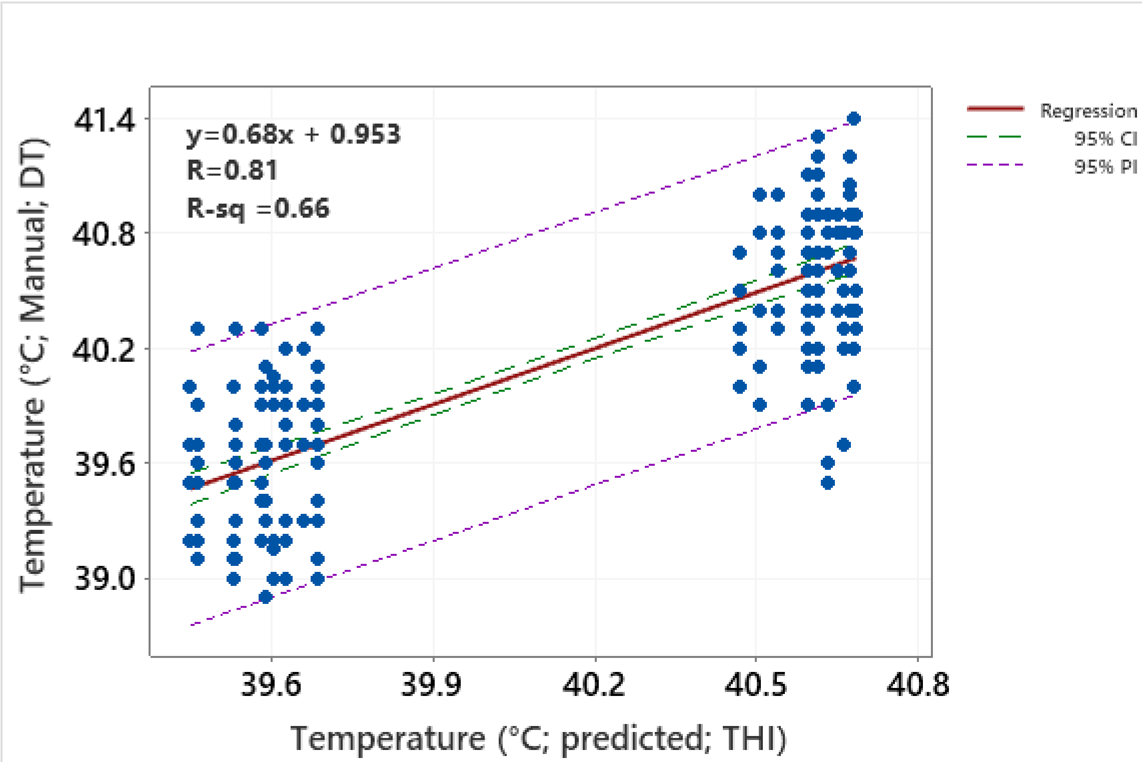

Fig 4. Comparing results from rectal temperatures measured manually using a digital thermometer vs. temperature predicted using linear regression fitted to THI-RT data. Abbreviations: R: Correlation, R^2: Coefficient of determination; CI: confidence interval; PI (prediction interval).

Table 2 shows the statistical data of the best models developed using various training algorithms. Overall, correlations from all models were highly significant with P<0.001. The scaled conjugate gradient algorithm with 7 neurons had the lowest R (0.87) and highest MSE (0.09; Table 2). However, models developed using Levenberg-Marquardt and BR algorithms with 10 neurons showed higher overall performance with R>0.90. Comparatively, BR showed the best performance with the least MSE (<0.05) with R values being consistently over 0.90 for all stages. Also, the BR model had the highest slope close to unity (b=0.83) when compared to others. Hence, according to these results, BR was selected as the best training algorithm for this network.

Table 2. Statistical results of the models developed using different algorithms.

Algorithm	Neurons	Stage	R	Slope (b)	MSE
Levenberg-Marquardt	10	Training	0.90	0.78	0.06
		Validation	0.93	0.77	0.09
		Testing	0.91	0.88	0.07

		Overall	0.90	0.79	0.05
Bayesian Regularization	10	Training	0.92	0.84	0.03
		Validation	-	-	-
		Testing	0.90	0.84	0.05
		Overall	0.92	0.83	0.02
Scaled Conjugate Gradient	7	Training	0.87	0.77	0.09
		Validation	0.87	0.76	0.09
		Testing	0.88	0.82	0.08
		Overall	0.87	0.78	0.07

R- correlation coefficient; MSE- mean square error.

Figure 5 shows the model's performance, with 10 hidden neurons, on the training, testing and overall data, which was trained with the BR algorithm. Better performance was found for the training stage (R=0.92; slope=0.84) while for the testing R= 0.90 and slope=0.84 and overall model had an R= 0.92, (R^2=0.85) and slope=0.83. The weights and biases in this model's hidden and output layers are available as supplementary material.

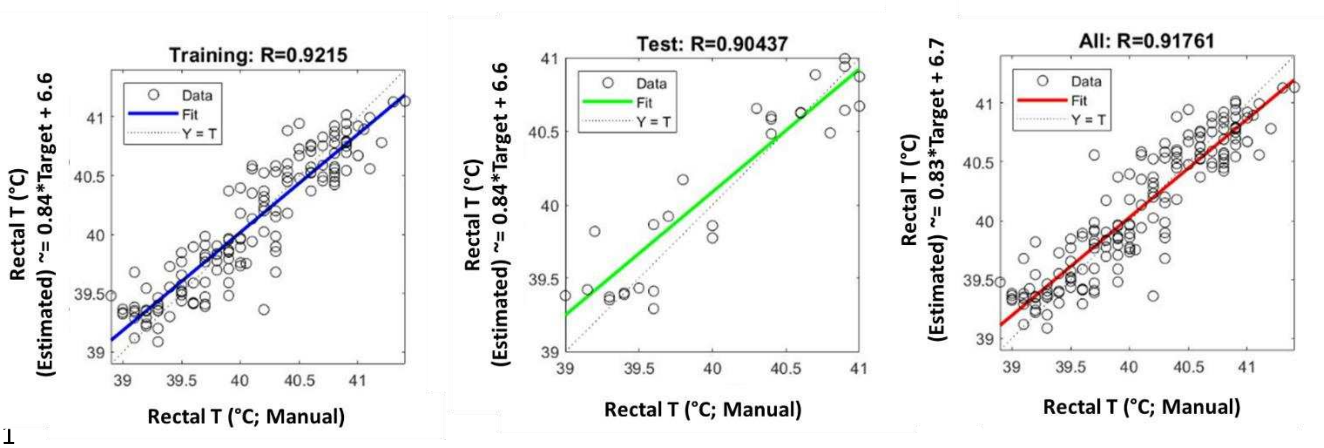

Fig 5. Comparison of the estimated and measured RT in training, test, and overall datasets, the neural network model was trained with the Bayesian Regularization algorithm to estimate rectal temperature from infrared thermal images (IRTIs) displaying the correlation coefficient (R) and 95% confidence bounds.

Figure 6 shows the linear regression model between RT measured manually and predicted temperature from the ANN model using IRT analysis. The linear regression model showed a high correlation (R=0.92) and coefficient of determination (R^2= 0.85) and was statistically significant (P<0.01) with slope=0.81. The model also showed 5.2% outliers (10 out of 192) based on the 95% confidence intervals.

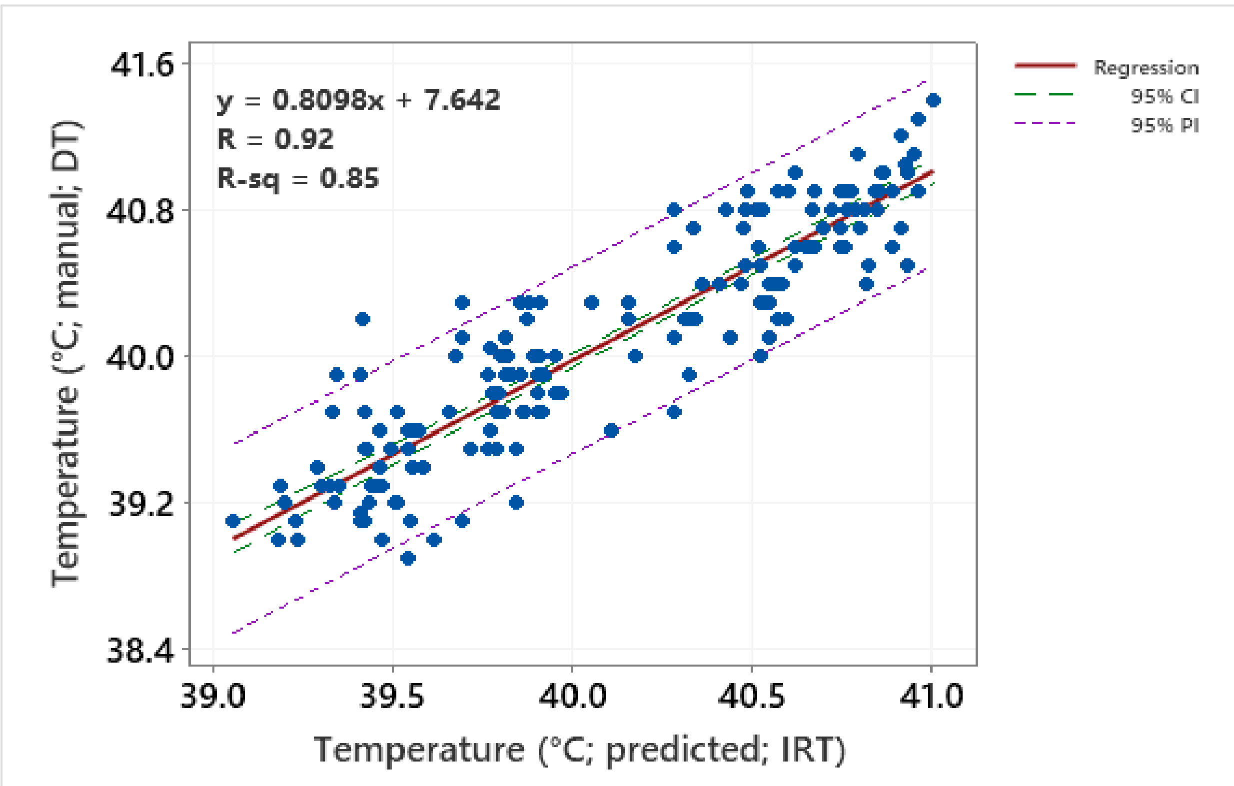

Fig 6. Linear regression model comparing results from rectal temperatures measured manually using a digital thermometer vs. temperature from the infrared thermal image analysis (IRT). Abbreviations: R^2: Coefficient of determination; CI: confidence interval; PI (prediction interval).

Figure 7 shows the PCA comparing RT measured manually (RT M), RT predicted using model (RT P), THI and skin temperatures of various ROIs obtained from IRT analysis for two sheep breeds (Dorper and SC) under both TN and HS conditions in different days of measurements. The PCA described 87.3% of the total data variability with 77.1% and 10.2% for PC1 and PC2, respectively. The results showed that RT M and RT P were closely related (Fig 7B). There was a clear difference in temperatures between HS and TN treatments such that the HS group showed higher THI and temperature values in both the breeds (Fig 7A).

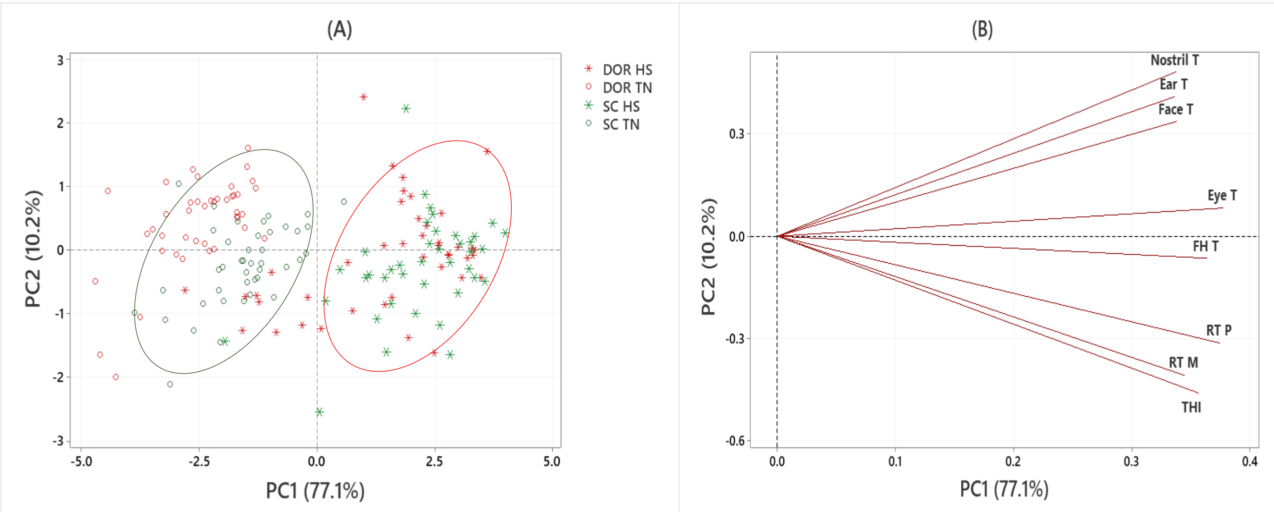

Fig 7. Principal components analysis: (A) Score plot and (B) Loading plot of data measured with (1) manual techniques (i) RT M: rectal temperature manual, (2) infrared thermal images (i) Nostril T: nostril temperature, (ii) Face T: face temperature, (iii) FH T: forehead temperature, (iv) Ear T: ear temperature (v) Eye T: eye temperature and those using the machine learning model (i) RT P: rectal temperature predicted from each day of the control and heat stress treatments for both Dorper and second cross sheep breeds.

Discussion

Infrared thermography has been used as a non-invasive remote sensing tool to assess changes in heat transfer and blood flow in ruminants via detecting slight variations in body temperature (Paim et al., 2012). Our study proposed selecting IRT of specific body locations such as the forehead, eye, muzzle, ear, and face, for estimating RT in sheep. The results demonstrated that THI and IRT, along with machine learning models, could help in the automated measurement of RT/body temperature in sheep to assess HS.

In recent years, with the growing awareness and interest of consumers in animal welfare, there is an urgent need to develop non-invasive measures of stress in animals to promote animal welfare. Producers and consumers are paying more attention to farm management conditions (Bittner et al., 2021) particularly on the procedures that prevent pain and discomfort. Thus, non-invasive techniques of measuring HS in ruminants such as IRT (Paim et al., 2012; McManus et al., 2015) and estimation of fecal cortisol metabolites (Rees et al., 2016) are gaining importance, but it demands further research for the optimization of the methods. In this current study, we used two different sheep breeds: 1) Dorpers with loose white hairy fleece with the head being free of wool and 2) SC breeds that had a chalky white dense fleece with a less wool in the forehead region (Joy et al., 2020b). Special care was taken while measuring FH T in SC to avoid wool interruptions.

Positive correlations among the IRTs, THI, and RT indicated that these variables were altered with a similar trend such that elevating THI corresponded to increasing RT and thermographic measurements (FH T, ear T, eye T, nostril T, and face T). The FH T and eye T showed the highest correlation with THI, suggesting that real-time monitoring of these regions may help to signify potential impacts of the increased environmental temperature on the thermoregulatory responses of sheep. This is in accordance with findings of previous studies (Daltro et al., 2017; Peng et al., 2019) that also indicated THI was highly correlated with FH T, and eye T in cattle. Also, RT showed a high correlation with FH T, eye T and nostril T. Measuring IRT of the eye region has been established as the best proxy of core body temperature in cattle (Daltro et al., 2017). There was also a moderate correlation between IRT of eyes and RT has been established in cattle (Gloster et al., 2011). Interestingly, nostril T showed a moderate correlation with the RT in sheep. This could be because the nose region in our study has more hairless skin exposed in sheep along with a large number of blood vessels (Dawes and Prichard, 1953), which allows measuring changes in blood flow and heat transfer more accurately.

Generally, the best ANN model is indicated by high correlation coefficient values (R) and training performance (MSE). To ensure that there is no overfitting, R and MSE values of the training and testing steps should be close to each other (Steyerberg et al., 2010). Considering a part of the data for validation before testing helps to reach this goal (Gonzalez Viejo et al., 2019). Although BR does not have a validation stage in particular, it has an implemented cross-validation which randomly divides the training data into training and validation and automatically trains the data several times until reaching the optimal combination of errors and weights using different sets of training data. This means the BR is more robust than the other algorithms (Taheri et al., 2021). Although THI showed a high correlation with RT, the observed correlations and determination coefficients of the model developed using THI as an input for predicting RT were relatively low. On the other hand, inclusion of IRT measurements as inputs improved the model performance and accuracy. Based on the performance of the three training algorithms applied for the model development, it can be concluded that BR with a NN structure of one hidden layer, containing 10 neurons with a tan-sigmoid transfer function was the most accurate for estimating RT using the IRT technique. This is based on the highest correlation coefficient (R=0.92), best performance (MSE= 0.02) for overall data, good fit within confidence bounds with a low number of outliers (5.2%), overall slope close to 1 (b=0.81), and fewer signs of overfitting. Similarly, Gonzalez Viejo et al. (2019) and Taheri et al. (2021) proved that BR was the most effective algorithm for training the neural network. The BR is a back-propagation algorithm based on Levenberg-Marquardt optimization, which works based on calculating the second derivatives of a cost function with an additional term for updating weights and biases (Tiwari et al., 2013) and minimizes a combination of squared errors and weights. Several studies stated some of the important advantages of BR over other training algorithms such as good generalization for small datasets (Kayri, 2016), avoids overfitting (Bruneau and McElroy, 2006), and does not require a separate validation stage (Gonzalez Viejo et al., 2019). However, this algorithm is slower and requires more memory than the Lavenberg-Marquardt training function (Tiwari et al., 2013; Taheri et al., 2021).

As expected, HS increased RT and IRTs in both sheep breeds, implying compromised thermoregulatory mechanisms in sheep exposed to high THI (Chauhan et al., 2016; Joy et al., 2020b). Further, there was a close association between THI, RT M and RT P obtained from PCA analysis which further indicates the acceptable precision of the proposed model in predicting RT of sheep under different THI conditions. Also, this model, if implemented, would be very useful in the remote monitoring of a large number of animals (i.e., at flock level), where the image/video is taken of the flock, but the data is analyzed for each animal individually (using image recognition software tools). As indicated before, the positioning of cameras, environmental conditions and excessive motion of animals could have an impact on applying these techniques under large scale conditions. Thus, further research is required to investigate the feasibility of implementing these techniques on at a flock scale and to reduce the impact of environmental factors on the accuracy. Additionally, the established model could be implemented in an intelligent interface to monitor the real-time sheep temperature on farms, which would allow a reduction in time and handling cost for producers while screening the stressed animals. Moreover, the implementation of artificial intelligence (AI) for automated data gathering using IRT images and video analysis will extend a reliable and completely automated system to identify stressed sheep during summer.

Conclusions

Infrared thermography measurements in sheep offer a reliable, precise, and non-invasive technique to measure HS. Among the ROIs studied using IRT, FH T and eye T showed the highest correlation with THI, and FHT, eye T, and nostril T were strongly correlated with RT. Further, a combination of IRT and machine learning techniques, namely ANN, was applied to model the RT in sheep. The best algorithm for the specific model developed in this current study was the BR with one hidden layer, containing 10 neurons with tangent sigmoid transfer function. The model showed the highest correlation (R=0.92) and least error (MSE=0.02). Therefore, it is concluded that IRT and machine learning could be used as a rapid and cost-effective technique to monitor real-time body temperatures in sheep for early detection of HS with minimal restraint to improve sheep welfare.

Conflict of interest

The authors declare no conflict of interest.

Acknowledgments

The authors would like to acknowledge The University of Melbourne for providing the Melbourne Graduate Research Scholarship to Aleena Joy, and School of Agriculture and Food, Faculty of Veterinary and Agricultural Sciences for giving startup fund to Dr. Surinder S. Chauhan to support this research.

References

Baida, B.E.L., Swinbourne, A.M., Barwick, J., Leu, S.T., van Wettere, W.H., 2021. Technologies for the automated collection of heat stress data in sheep. Animal Biotelemetry 9, 1-15.

Bittner, E., Ashman, H., van Barneveld, R., McNamara, A., Thomson, N., Hearn, A., Dunshea, F., 2021. Qualitative assessment of value in Australian pork across cultures. Anim. Prod. Sci. https://doi.org/10.1071/AN21011

Brown-Brandl, T., Eigenberg, R., Hahn, G., Nienaber, J., 1999. Measurements of bioenergetic responses in livestock. ASAE Meeting Presentation Paper No. 994210. St. Joseph, ASAE, USA.

Bruneau, P., McElroy, N.R., 2006. logD 7.4 modeling using Bayesian regularized neural networks. Assessment and correction of the errors of prediction. J. Chem. Inf. Model. 46, 1379-1387.

Chauhan, S., Celi, P., Fahri, F., Leury, B., Dunshea, F., 2014a. Dietary antioxidants at supranutritional doses modulate skeletal muscle heat shock protein and inflammatory gene expression in sheep exposed to heat stress. J. Anim. Sci. 92, 4897-4908.

Chauhan, S.S., Celi, P., Leury, B.J., Clarke, I.J., Dunshea, F.R., 2014b. Dietary antioxidants at supranutritional doses improve oxidative status and reduce the negative effects of heat stress in sheep. J. Anim. Sci. 92, 3364-3374.

Chauhan, S., Ponnampalam, E., Celi, P., Hopkins, D., Leury, B., Dunshea, F., 2016. High dietary vitamin E and selenium improves feed intake and weight gain of finisher lambs and maintains redox homeostasis under hot conditions. Small Rumin. Res. 137, 17-23.

Chauhan, S.S., Rashamol, V., Bagath, M., Sejian, V., Dunshea, F.R., 2021. Impacts of heat stress on immune responses and oxidative stress in farm animals and nutritional strategies for amelioration. Int. J. Biometeorol., 1-14.

Daltro, D.d.S., Fischer, V., Alfonzo, E.P.M., Dalcin, V.C., Stumpf, M.T., Kolling, G.J., Silva, M.V.G.B.d., McManus, C., 2017. Infrared thermography as a method for evaluating the heat tolerance in dairy cows. Rev. Bras. Zootecn. 46, 374-383.

Dawes, J., Prichard, M.M., 1953. Studies of the vascular arrangements of the nose. J. Anat. 87, 311.

FLIRSystems, 2015. FLIR Systems, Inc. Corporate Headquarters 27700 SW Parkway Ave. Wilsonville, OR 97070 USA.

Fuentes, A., Yoon, S., Park, J., Park, D.S., 2020a. Deep learning-based hierarchical cattle behavior recognition with spatio-temporal information. Computers and Electronics in Agriculture 177, 105627.

Fuentes, S., Gonzalez Viejo, C., Chauhan, S.S., Joy, A., Tongson, E., Dunshea, F.R., 2020b. Non-Invasive Sheep Biometrics Obtained by Computer Vision Algorithms and Machine Learning Modeling Using Integrated Visible/Infrared Thermal Cameras. Sensors 20, 6334.

Fuentes, S., Gonzalez Viejo, C., Cullen, B., Tongson, E., Chauhan, S.S., Dunshea, F.R., 2020c. Artificial Intelligence Applied to a Robotic Dairy Farm to Model Milk Productivity and Quality based on Cow Data and Daily Environmental Parameters. Sensors 20, 2975.

Gloster, J., Ebert, K., Gubbins, S., Bashiruddin, J., Paton, D.J., 2011. Normal variation in thermal radiated temperature in cattle: implications for foot-and-mouth disease detection. BMC Vet. Res. 7, 1-10.

Gonzalez Viejo, C., Torrico, D.D., Dunshea, F.R., Fuentes, S., 2019. Development of artificial neural network models to assess beer acceptability based on sensory properties using a robotic pourer: a comparative model approach to achieve an artificial intelligence system. Beverages 5, 33.

Goodwin, S.D., 1998. Comparison of body temperatures of goats, horses, and sheep measured with a tympanic infrared thermometer, an implantable microchip transponder, and a rectal thermometer. Journal of the American Association for Laboratory Animal Science 37, 51-55.

Hillman, P., Gebremedhin, K., Willard, S., Lee, C., Kennedy, A., 2009. Continuous measurements of vaginal temperature of female cattle using a data logger encased in a plastic anchor. Applied Engineering in agriculture 25, 291-296.

Hoffmann, G., Schmidt, M., Ammon, C., Rose-Meierhöfer, S., Burfeind, O., Heuwieser, W., Berg, W., 2013. Monitoring the body temperature of cows and calves using video recordings from an infrared thermography camera. Vet. Res. Commun. 37, 91-99.

Idris, M., Uddin, J., Sullivan, M., McNeill, D.M., Phillips, C.J., 2021. Non-Invasive Physiological Indicators of Heat Stress in Cattle. Animals 11, 71.

Ipema, A., Goense, D., Hogewerf, P., Houwers, H., Van Roest, H., 2008. Pilot study to monitor body temperature of dairy cows with a rumen bolus. Computers and Electronics in Agriculture 64, 49-52.

Jorquera-Chavez, M., Fuentes, S., Dunshea, F.R., Warner, R.D., Poblete, T., Jongman, E.C., 2019. Modelling and validation of computer vision techniques to assess heart rate, eye temperature, ear-base temperature and respiration rate in cattle. Animals 9, 1089.

Joy, A., Dunshea, F.R., Leury, B.J., Clarke, I.J., DiGiacomo, K., Chauhan, S.S., 2020a. Resilience of small ruminants to climate change and increased environmental temperature: A review. Animals 10, 867.

Joy, A., Dunshea, F.R., Leury, B.J., DiGiacomo, K., Clarke, I.J., Zhang, M.H., Abhijith, A., Osei-Amponsah, R., Chauhan, S.S., 2020b. Comparative Assessment of Thermotolerance in Dorper and Second-Cross (Poll Dorset/Merino× Border Leicester) Lambs. Animals 10, 2441.

Kayri, M., 2016. Predictive abilities of bayesian regularization and Levenberg–Marquardt algorithms in artificial neural networks: a comparative empirical study on social data. Mathematical and Computational Applications 21, 20.

Koluman, N., Daskiran, I., 2011. Effects of ventilation of the sheep house on heat stress, growth and thyroid hormones of lambs. Trop. Anim. Health Prod. 43, 1123-1127.

Lees, A.M., Sejian, V., Lees, J., Sullivan, M., Lisle, A., Gaughan, J., 2019. Evaluating rumen temperature as an estimate of core body temperature in Angus feedlot cattle during summer. Int. J. Biometeorol. 63, 939-947.

Macmillan, K., Colazo, M., Cook, N., 2019. Evaluation of infrared thermography compared to rectal temperature to identify illness in early postpartum dairy cows. Res. Vet. Sci. 125, 315-322.

Marai, I., El-Darawany, A., Fadiel, A., Abdel-Hafez, M., 2007. Physiological traits as affected by heat stress in sheep—a review. Small Rumin. Res. 71, 1-12.

Marai, I.F.M., El-Darawany, A., Fadiel, A., Abdel-Hafez, M., 2008. Reproductive performance traits as affected by heat stress and its alleviation in sheep. Trop. Subtrop. Agroecosystems 8, 209-234.

Maurya, V., Sejian, V., Kumar, D., Naqvi, S., 2016. Impact of heat stress, nutritional restriction and combined stresses (heat and nutritional) on growth and reproductive performance of Malpura rams under semi-arid tropical environment. J. Anim. Physiol. Anim. Nutr. (Berl.) 100, 938-946.

McManus, C., Bianchini, E., Paim, T.D.P., De Lima, F.G., Neto, J.B., Castanheira, M., Esteves, G.I.F., Cardoso, C.C., Dalcin, V.C., 2015. Infrared thermography to evaluate heat tolerance in different genetic groups of lambs. Sensors 15, 17258-17273.

Metzner, M., Sauter-Louis, C., Seemueller, A., Petzl, W., Klee, W., 2014. Infrared thermography of the udder surface of dairy cattle: Characteristics, methods, and correlation with rectal temperature. The Veterinary Journal 199, 57-62.

Montanholi, Y.R., Odongo, N.E., Swanson, K.C., Schenkel, F.S., McBride, B.W., Miller, S.P., 2008. Application of infrared thermography as an indicator of heat and methane production and its use in the study of skin temperature in response to physiological events in dairy cattle (Bos taurus). J. Therm. Biol. 33, 468-475.

Osei-Amponsah, R., Chauhan, S.S., Leury, B.J., Cheng, L., Cullen, B., Clarke, I.J., Dunshea, F.R., 2019. Genetic Selection for Thermotolerance in Ruminants. Animals 9, 948.

Osei-Amponsah, R., Dunshea, F.R., Leury, B.J., Cheng, L., Cullen, B., Joy, A., Abhijith, A., Zhang, M.H., Chauhan, S.S., 2020. Heat Stress Impacts on Lactating Cows Grazing Australian Summer Pastures on an Automatic Robotic Dairy. Animals 10, 869.

Paim, T.d.P., Borges, B.O., Lima, P., Dallago, B., Louvandini, H., McManus, C., 2012. Relation between thermographic temperatures of lambs and thermal comfort indices. Int. J. Appl. Anim. Sci 1, 108-115.

Peng, D., Chen, S., Li, G., Chen, J., Wang, J., Gu, X., 2019. Infrared thermography measured body surface temperature and its relationship with rectal temperature in dairy cows under different temperature-humidity indexes. Int. J. Biometeorol. 63, 327-336.

Phillips, C., 2016. The welfare risks and impacts of heat stress on sheep shipped from Australia to the Middle East. The Veterinary Journal 218, 78-85.

Rees, A., Fischer-Tenhagen, C., Heuwieser, W., 2016. Effect of heat stress on concentrations of faecal cortisol metabolites in dairy cows. Reproduction in Domestic Animals 51, 392-399.

Salles, M.S.V., da Silva, S.C., Salles, F.A., Roma Jr, L.C., El Faro, L., Mac Lean, P.A.B., de Oliveira, C.E.L., Martello, L.S., 2016. Mapping the body surface temperature of cattle by infrared thermography. J. Therm. Biol. 62, 63-69.

Shi, L., Xu, Y., Mao, C., Wang, Z., Guo, S., Jin, X., Yan, S., Shi, B., 2020. Effects of heat stress on antioxidant status and immune function and expression of related genes in lambs. Int. J. Biometeorol. 64, 2093-2104.

Stelletta, C., Gianesella, M., Vencato, J., Fiore, E., Morgante, M., 2012. Thermographic applications in veterinary medicine. Infrared Thermography. In Tech, China, 117-140. ISBN: 978-953-51-0232-7. Available from: http://www.intechopen.com/books/infrared thermography/thermographic-applications-in-veterinary-medicine.

Stewart, M., Wilson, M., Schaefer, A., Huddart, F., Sutherland, M., 2017. The use of infrared thermography and accelerometers for remote monitoring of dairy cow health and welfare. J. Dairy Sci. 100, 3893-3901.

Steyerberg, E.W., Vickers, A.J., Cook, N.R., Gerds, T., Gonen, M., Obuchowski, N., Pencina, M.J., Kattan, M.W., 2010. Assessing the performance of prediction models: a framework for some traditional and novel measures. Epidemiology (Cambridge, Mass.) 21, 128.

Taheri, S., Brodie, G., Gupta, D., 2021. Optimised ANN and SVR models for online prediction of moisture content and temperature of lentil seeds in a microwave fluidised bed dryer. Computers and Electronics in Agriculture 182, 106003.

Tiwari, S., Naresh, R., Jha, R., 2013. Comparative study of backpropagation algorithms in neural network based identification of power system. International Journal of Computer Science & Information Technology 5, 93.

Zhang, M., Warner, R.D., Dunshea, F.R., DiGiacomo, K., Joy, A., Abhijith, A., Osei-Amponsah, R., Hopkins, D.L., Ha, M., Chauhan, S.S., 2021. Impact of heat stress on the growth performance and retail meat quality of 2nd cross (Poll Dorset × (Border Leicester × Merino)) and Dorper lambs. Meat Sci. 181, 108581. https://doi.org/10.1016/j.meatsci.2021.108581.